AMERICAN SOCIETY FOR MICROBIOLOGY | Journal of Virology®

VIRUS-CELL INTERACTIONS

The Interferon-Inducible Proteoglycan Testican-2/SPOCK2 Functions as a Protective Barrier against Virus Infection of Lung Epithelial Cells

Narae Ahn,[a] Woo-Jong Kim,[a] Nari Kim,[a,b] Han Wook Park,[c] Seung-Woo Lee,[a,b,c] Joo-Yeon Yoo[a,b]

[a]Department of Life Sciences, Pohang University of Science and Technology, Pohang, Republic of Korea
[b]Organelle Network Research Center, Pohang University of Science and Technology, Pohang, Republic of Korea
[c]Department of Integrative Biosciences & Biotechnology, Pohang University of Science and Technology, Pohang, Republic of Korea

ABSTRACT Proteoglycans function not only as structural components of the extracellular compartment but also as regulators of various cellular events, including cell migration, inflammation, and infection. Many microbial pathogens utilize proteoglycans to facilitate adhesion and invasion into host cells. Here we report a secreted form of a novel heparan sulfate proteoglycan that functions against virus infection. The expression of SPOCK2/testican-2 was significantly induced in virus-infected lungs or in interferon (IFN)-treated alveolar lung epithelial cells. Overexpression from a SPOCK2 expression plasmid alone or the treatment of cells with recombinant SPOCK2 protein efficiently blocked influenza virus infection at the step of viral attachment to the host cell and entry. Moreover, mice treated with purified SPOCK2 were protected against virus infection. Sialylated glycans and heparan sulfate chains covalently attached to the SPOCK2 core protein were critical for its antiviral activity. Neuraminidase (NA) of influenza virus cleaves the sialylated moiety of SPOCK2, thereby blocking its binding to the virus. Our data suggest that IFN-induced SPOCK2 functions as a decoy receptor to bind and block influenza virus infection, thereby restricting entry of the infecting virus into neighboring cells.

IMPORTANCE Here we report a novel proteoglycan protein, testican-2/SPOCK2, that prevents influenza virus infection. Testican-2/SPOCK2 is a complex type of secreted proteoglycan with heparan sulfate GAG chains attached to the core protein. SPOCK2 expression is induced upon virus infection or by interferons, and the protein is secreted to an extracellular compartment, where it acts directly to block virus-cell attachment and entry. Treatment with purified testican-2/SPOCK2 protein can efficiently block influenza virus infection *in vitro* and *in vivo*. We also identified the heparan sulfate moiety as a key regulatory module for this inhibitory effect. Based on its mode of action (cell attachment/entry blocker) and site of action (extracellular compartment), we propose testican-2/SPOCK2 as a potential antiviral agent that can efficiently control influenza virus infection.

KEYWORDS antiviral, extracellular matrix, influenza, SPOCK2, proteoglycan

Interferons (IFNs) play central roles in the regulation of innate and adaptive immune responses against virus infection (1). Upon the detection of extra- or intracellular virus by the host innate defense system, IFNs are secreted to activate JAK-STAT-mediated signaling pathways and transcribe hundreds of interferon-stimulated genes (ISGs). The antiviral functions of IFNs can be elucidated by the combined activities of ISGs, which include pathogen recognition receptors, regulators of antiviral signaling pathways, and antiviral effector molecules. In contrast to many ISGs that help the host become sensitized to or enhance its capacity to defend against infection, a few ISGs can act directly on viruses

Citation Ahn N, Kim W-J, Kim N, Park HW, Lee S-W, Yoo J-Y. 2019. The interferon-inducible proteoglycan testican-2/SPOCK2 functions as a protective barrier against virus infection of lung epithelial cells. J Virol 93:e00662-19. https://doi.org/10.1128/JVI.00662-19.

Editor Bryan R. G. Williams, Hudson Institute of Medical Research

Address correspondence to Joo-Yeon Yoo, jyoo@postech.ac.kr.

Received 23 April 2019
Accepted 16 July 2019
Accepted manuscript posted online 24 July 2019
Published 30 September 2019

to block viral entry or replication. Considering the therapeutic potential of this approach to combat virus infection, the identification and characterization of novel effector ISGs that act directly on viruses are important (2, 3).

Virus infection begins with the attachment of the virus to receptors on the host cell surface. Most of the viral envelope is coated with glycoproteins, and the interaction between the viral glycoproteins, such as sialylated glycans or glycosaminoglycans (GAGs), and the host cell surface receptors initiates virus infection, followed by membrane fusion and entry. The α2,3- and α2,6-linked sialylated glycans on the surface of lung epithelial cells function as the attachment receptors for influenza virus, while heparan sulfate serves as the host receptor for a diverse array of viruses, such as herpes simplex virus, dengue virus, human immunodeficiency virus (HIV), and hepatitis C virus (HCV) (4–7). Most of the heparan sulfate on the cell surface or in the extracellular matrix (ECM) is attached to proteins called proteoglycans. Proteoglycans are heavily glycosylated proteins with a core protein unit and covalently attached chains of GAGs such as heparan sulfate, chondroitin sulfate, and keratin sulfate (8). Proteoglycans also serve as coreceptors for cytokines, chemokines, and growth factors to function during inflammation, tissue repair, and development (9).

SPOCK (SPARC/osteonectin CWCV and Kazal-like domains), also known as testican, is a secreted proteoglycan with three known homologs, SPOCK1, -2, and -3. SPOCK was initially characterized as a progenitor form of a seminal plasma GAG-bearing peptide and was later cloned and identified as a chondroitin/heparan sulfate proteoglycan (HSPG). Although originally identified in the testicles, SPOCK1, -2, and -3 mRNAs are highly expressed in the brain, and their neuronal functions have been studied (10–12). The SPOCK1 and -2 proteoglycans inhibit neuronal cell attachment and neurite extension, while *Spock3*$^{-/-}$ mice exhibit structural abnormalities in the brain that are linked to abnormal behavior. In the ECM, SPOCK1 and SPOCK3 inactivate membrane-type matrix metalloproteinases (MT-MMPs), but these inhibitory effects are abrogated by SPOCK2, indicating that the interplay between testican/SPOCK proteoglycan family members contributes to the proteoglycan-rich extracellular environment of the central nervous system and the regulation of neurogenesis (13).

SPOCK2 mRNA is detected in the lung. Moreover, polymorphism in SPOCK2 was recently identified as a genetic trait linked to susceptibility to bronchopulmonary dysplasia, a chronic respiratory disease common among premature infants (6). In this report, we address the protective role of SPOCK2 in defense against virus infection. We examined the induction of SPOCK2 mRNA and protein during virus infection in the mouse lung and in type II alveolar epithelial cell (AEC)-derived A549 cells. This report explores the molecular mechanism as well as the physiological significance of the IFN-inducible, secretory proteoglycan SPOCK2 in the host defense against virus infection.

RESULTS

SPOCK2 expression is induced by virus infection in the lung. Based on the basal expression patterns in the lung and the genetic association with bronchopulmonary dysplasia, we wondered whether SPOCK2 expression changes during lung injury. To test this hypothesis, we examined SPOCK2 expression during lung injury induced by virus infection (Fig. 1A). BALB/c mice were intranasally inoculated with two different titers of influenza virus strain A/Puerto Rico/8/34 (PR8), and the expression of SPOCK2 mRNA in the lung was evaluated by quantitative real-time PCR (qRT-PCR) at days 2 and 7 postinfection. Virus infection significantly enhanced SPOCK2 mRNA expression in the lung at day 2 postinfection and then slightly decreased SPOCK2 mRNA expression in the lung at day 7. Similar patterns were detected for SPOCK2 protein expression in the lungs of the infected mice (Fig. 1B). Next, we examined whether SPOCK2 induction could be similarly observed in virus-infected A549 human type II AECs. The SPOCK2 protein level increased to a maximum at 6 h postinfection and then declined (Fig. 1C). Interestingly, endogenous SPOCK2 was observed as doublets, and only the lower bands were increased upon virus infection.

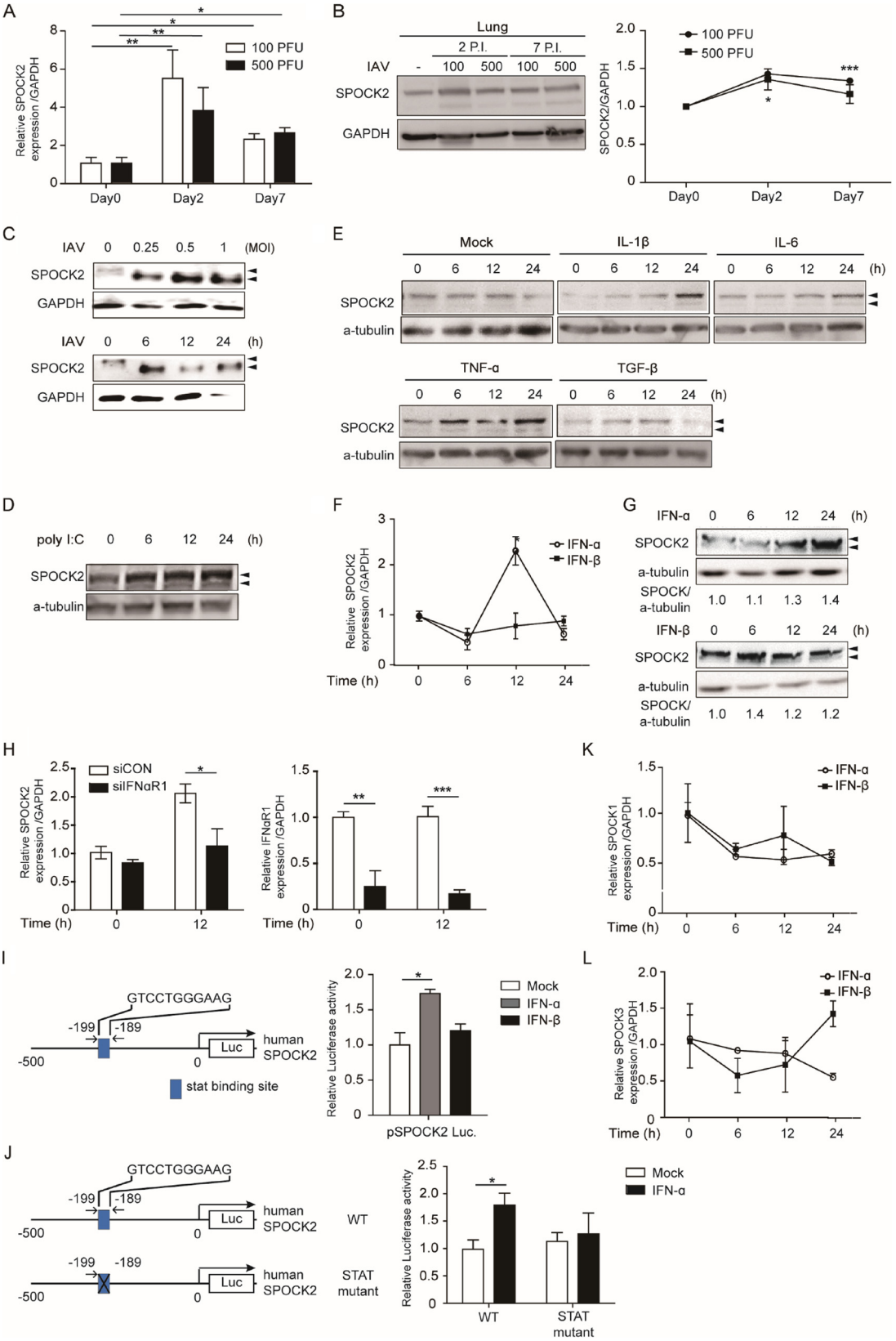

FIG 1 Induction of SPOCK2 expression by IFNs, poly(I·C), and virus. (A and B) Nine-week-old mice were infected with 100 or 500 PFU of PR8 IAV. (A) The expression of SPOCK2 mRNA in the lungs of infected mice was detected by quantitative RT-PCR (qRT-PCR). The experiment was performed in triplicate, and the mean fold is indicated relative to the control group. Each bar indicates the average value ± SD obtained from triplicate experiments. Statistically significant differences from the controls, calculated using

(Continued on next page)

To mimic virus infection, a viral RNA (vRNA) analog, poly(I·C), was transfected into cells, and the dynamics of SPOCK2 expression were measured. The intracellular transfection of poly(I·C) induced SPOCK2 similarly to influenza virus, with slightly different kinetics (Fig. 1D). These results indicate that SPOCK2 expression might be controlled by the secondary signal induced by infection but not by the virus itself. To test this hypothesis, A549 cells were stimulated with various inflammatory cytokines secreted during virus infection, and SPOCK2 protein levels were determined by Western blotting (WB). Among the tested cytokines, interleukin 1β (IL-1β), IL-6, and IFN-α were the most effective at inducing SPOCK2 expression (Fig. 1E and G). Although IFN-α and IFN-β belong to the same type I IFN family and utilize the same type I IFN receptors, treatment with IFN-α but not IFN-β significantly induced the expression of SPOCK2 mRNA and protein (Fig. 1F and G). As IFN-α and IFN-β have different binding affinities for IFN-α/β receptors 1 and 2 (IFNAR1 and -2) and induce distinct ISGs, these results suggest that SPOCK2 belongs to a set of ISGs that are differentially regulated by IFN-α and -β (14–16). To verify that the expression of SPOCK2 by virus infection is IFN dependent, we next measured SPOCK2 expression in IFNAR1-silenced cells. Significantly reduced SPOCK2 mRNA expression was detected in IFNAR1-silenced cells upon virus infection, suggesting that IFN-mediated signaling activity is required to induce SPOCK2 expression (Fig. 1H). The SPOCK2 promoter possesses one STAT binding site, predicted by both the UCSC genome browser and the JASPAR database. Therefore, we directly assessed its responsiveness to IFN by generating a luciferase construct fused with a 0.5-kb genomic DNA fragment spanning the promoter region of human SPOCK2 (Fig. 1I). The luciferase assay with the SPOCK2 promoter reporter construct clearly demonstrated that IFNα directly activates SPOCK2 gene expression. When the putative STAT binding site within the promoter of SPOCK2 was mutated, IFN-mediated induction of luciferase activity disappeared, confirming that SPOCK2 expression is directly induced by IFN-α.

In addition to that of SPOCK2, SPOCK1 expression at the mRNA and protein levels was increased in human non-small-cell lung cancer (NSCLC) tissues and cell lines (17). SPOCK1 is also reported to regulate lung cancer cells during the epithelial-to-mesenchymal transition (18). SPOCK3 is reported to be induced during lung development and lung-directed differentiation (19). Thus, we examined whether the expression of other SPOCK family members changed upon IFN-α or IFN-β treatment in A549 cells. In contrast to SPOCK2 expression, however, the expression of neither SPOCK1 nor SPOCK3 was significantly altered by treatment with either IFN-α or IFN-β (Fig. 1J and K).

Overexpressed SPOCK2 inhibits virus infection. ISGs induced upon virus infection usually function in the host defense against infection. To examine whether SPOCK2 plays any regulatory role during virus infection, various titers of influenza virus were

FIG 1 Legend (Continued)
the *t* test, are indicated as follows: *, $P < 0.05$, and **, $P < 0.01$. (B) Proteins in the lungs of infected mice were detected by immunoblotting with anti-SPOCK2 and anti-GAPDH. Intensity values were quantified using the Multigauge program (Fuji Film). Each bar indicates the average value ± SD obtained from triplicate experiment. Statistically significant differences from the controls, calculated using the *t* test, are indicated as follows: *, $P < 0.05$, and ***, $P < 0.001$. P.I., days postinfection. (C) A549 cells were infected with PR8 IAV at the indicated dose (top) or for the indicated time (bottom). Immunoblots of cell extracts were probed with anti-SPOCK2 and with anti-GAPDH antibodies as a loading control. (D and E) A549 cells were transfected with 1 μg of poly(I·C) (D) or incubated with IL-1β (20 ng/ml), IL-6 (20 ng/ml), TNF-α (20 ng/ml), or TGF-β (20 ng/ml) (E) at the indicated time. Cell extracts were immunoblotted with anti-SPOCK2 and anti-GAPDH antibodies used as a loading control. (F, K, and L) Indicated subtypes of SPOCK mRNA levels were measured by qRT-PCR at the indicated time points after treatment with human IFN-α (100 U/ml) or IFN-β (100 U/ml) in A549 cells. Expression was normalized to that of GAPDH. Each bar indicates the average value ± SD obtained from triplicate experiments. *, $P < 0.05$ compared with the control (*t* test). (G) A594 cells were treated with human IFN-α (100 U/ml) or IFN-β (100 U/ml) for the indicated time. Cell extracts were immunoblotted with anti-SPOCK2 and with anti-GAPDH antibodies as a loading control. (H) A549 cells were transfected with control siRNA or IFN-αR1 siRNA. After 20 h, the cells were infected with PR8 IAV (MOI, 1) for 12 h. SPOCK2, IFN-αR1, and GAPDH levels were determined by qRT-PCR. The graph presents the average values from triplicate experiments. Error bars represent SDs. *, $P < 0.05$; **, $P < 0.01$; ***, $P < 0.001$ for the control and SPOCK2 siRNA-transfected cells (*t* test). (I and J) (Left) Diagram of the pSPOCK2-luc construct, the 0.5-kb genomic DNA fragment of SPOCK2, with or without predicted STAT binding sites. (Right) A549 cells were transfected with pSPOCK2-luc and pRL-TK. After 36 h of transfection, the A549 cells were treated with human IFN-α (100 U/ml) or IFN-β (100 U/ml). After 12 h, the dual-luciferase assay was performed. "Mock" indicates samples treated with distilled water-treated. The graphs present the average values from triplicate experiments. Error bars represent SDs. *, $P < 0.05$ compared to mock (*t* test).

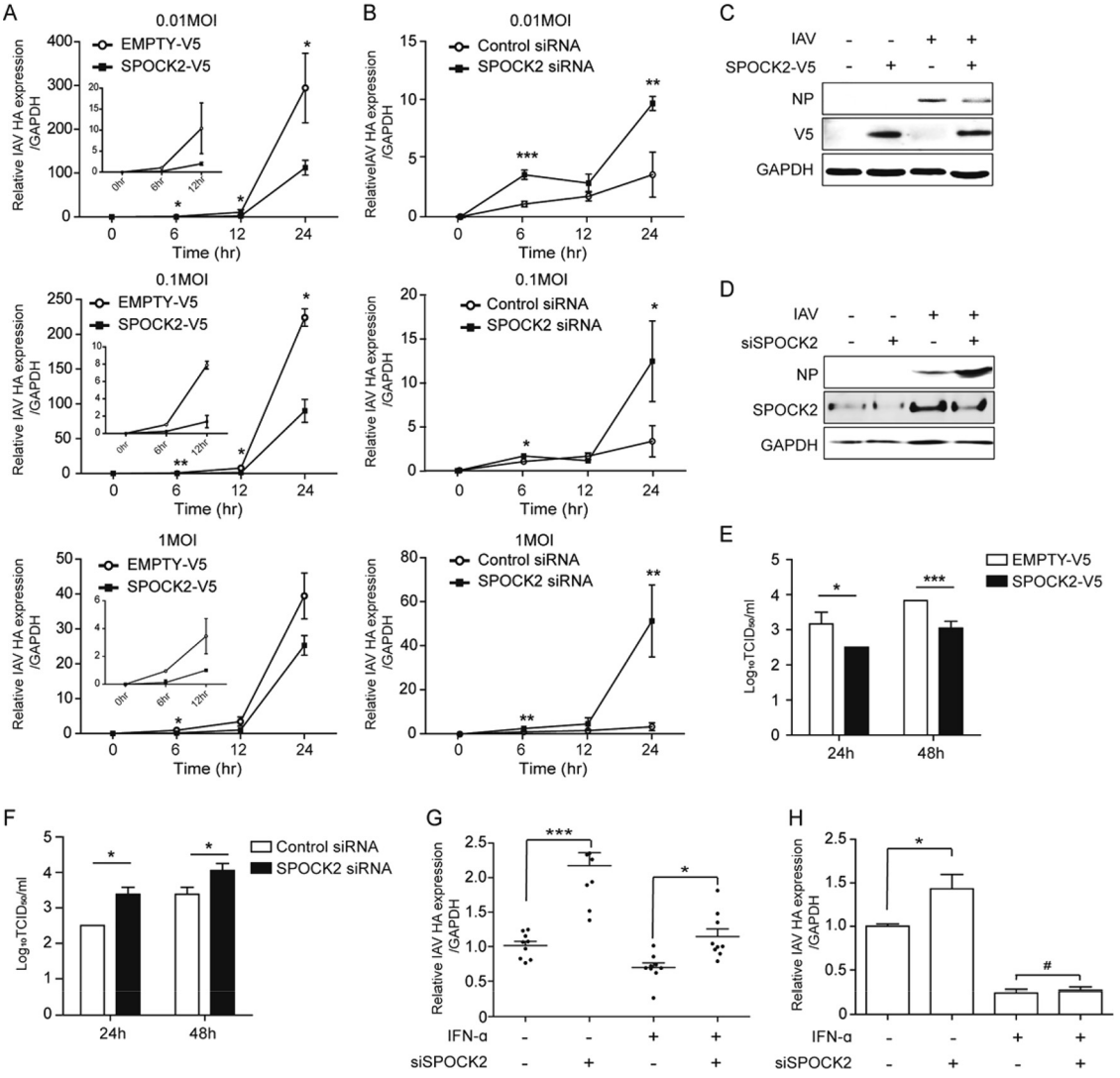

FIG 2 SPOCK2 inhibits influenza virus infection. (A) A549 cells were transfected with V5-tagged SPOCK2 or empty vector. After 24 h, the cells were infected with PR8 IAV (MOIs, 0.01, 0.1, and 1) for the indicated times. HA vRNA levels were measured by qRT-PCR. Expression was normalized to GAPDH. In the graph, HA expression at 6 h in the EMPTY-V5-transfected sample was set to 1 at each dose. The graph presents the average values from triplicate experiments. Error bars represent SDs. *, $P < 0.05$; **, $P < 0.01$; ***, $P < 0.001$ for comparison between EMPTY-V5- and SPOCK2-V5-transfected cells (*t* test). (B) A549 cells were transfected with control siRNA or SPOCK2 siRNA. After 24 h, the cells were infected with PR8 IAV (MOI, 0.01, 0.1, and 1) for the indicated times. After another 24 h, HA vRNA and GAPDH levels were determined by qRT-PCR. In the graph, HA expression at 6 h in the control siRNA-transfected sample was set to 1 at each dose. The graph presents the average values from triplicate experiments. Error bars represent SDs. *, $P < 0.05$; **, $P < 0.01$ for comparison between the control and SPOCK2 siRNA-transfected cells (*t* test). (C and D) Cell lysates from SPOCK2-V5-overexpressing (C) or SPOCK2-silenced (D) cells infected with PR8 IAV for 12 h (MOI, 1) were analyzed with anti-NP and anti-V5, anti-SPOCK2, and anti-GAPDH as a loading control. (E and F) At 36 h posttransfection, A549 cells were infected with IAV at an MOI of 1 for 24 h or 48 h. The supernatants from infected A549 cells were collected, and the viral titers were measured by the $TCID_{50}$ method. A549 cells were transfected with the V5-tagged SPOCK2 plasmid and the indicated siRNA (F). The bars indicate the mean values ± SDs obtained from three experiments. (G and H) A549 cells (G) and HEK293 cells (H) were transfected with control siRNA or SPOCK2 siRNA. After 24 h, the cells were infected for 12 h after treatment with IFN-α (100 U) for 16 h. HA vRNA levels were measured by qRT-PCR. Expression was normalized to that of GAPDH. Each graph presents mean data from three independent experiments, and error bars indicate SEMs. *, $P < 0.05$; **, $P < 0.01$; ***, $P < 0.001$; #, $P > 0.05$ (not significant) (*t* test).

applied to SPOCK2-overexpressing or SPOCK2-silenced A549 cells, and the amount of intracellular virus was measured. For every virus titer tested, SPOCK2 overexpression significantly lowered the intracellular levels of influenza hemagglutinin (HA) RNA and nucleoprotein (NP) protein expression (Fig. 2A and C). In addition, the intracellular levels of influenza virus were significantly enhanced in the SPOCK2-silenced A549 cells (Fig. 2B and D), indicating that SPOCK2 exerts an antiviral function during infection. Next, we infected SPOCK2-overexpressing or SPOCK2-silenced A549 cells with serial

dilutions of the influenza virus PR8 strain and calculated the 50% tissue culture infective dose ($TCID_{50}$) by measuring the viral titer (Fig. 2E and F). SPOCK2 overexpression resulted in a reduction in the $TCID_{50}$, while SPOCK2 silencing exhibited the reverse effect. Together, these results suggest that SPOCK2 has a host-protective effect against influenza virus infection in lung epithelial cells.

To confirm whether the induction of SPOCK2 expression by interferons truly contributes to the inhibition of influenza virus infection, we measured HA expression after IFN-α treatment in the presence or absence of SPOCK2 expression. Higher levels of HA expression were measured in the control cells than in the SPOCK2-silenced A549 cells, suggesting that the induction of SPOCK2 expression by IFN plays an important role in the control of influenza virus infection (Fig. 2G). Although we observed a clear SPOCK2 effect in these cells, the antiviral effect of IFN was not dramatic. Therefore, we chose HEK293 cells, in which IFN treatment markedly inhibits influenza virus infection. In these cells, the effect of SPOCK2 silencing on virus infection was still observed, although it was less efficient than the effect on A549 cells. However, the effect of SPOCK2 almost completely disappeared following cotreatment with IFN, confirming that induction of SPOCK2 by IFN plays a role in the control of influenza virus infection (Fig. 2H).

Treatment with recombinant SPOCK2 protein protects the host against influenza virus infection. Since SPOCK2 is a secreted proteoglycan, our data so far indicate that SPOCK2 might accumulate in the extracellular compartment to act on both its host cells and neighboring cells. Therefore, we hypothesized that the direct application of SPOCK2 protein in the extracellular compartment would exert antiviral effects. To test this hypothesis, cultured medium from SPOCK2-overexpressing CHO cells was applied to A549 cells, along with influenza virus (Fig. 3A). With increasing doses of the cultured medium from SPOCK2-overexpressing cells, the intracellular viral HA level decreased, confirming that antiviral SPOCK2 is secreted and present in the extracellular compartment (Fig. 3B). To test whether SPOCK2 pretreatment prevents virus infection, SPOCK2-containing culture medium was applied to A549 cells 3 h before virus infection (Fig. 3A). To avoid possible contamination, the SPOCK2-containing culture medium was washed and replaced with fresh culture medium. In contrast to the cotreatment condition, however, SPOCK2 pretreatment did not effectively block virus infection (Fig. 3C). Additionally, no antiviral activity of SPOCK2 was observed when culture medium was administered after virus infection (Fig. 3D). These results indicate that SPOCK2 was effective only when applied simultaneously with the virus.

To confirm that extracellular SPOCK2 proteins function to inhibit virus infection, recombinant human His-SPOCK2 proteins were purified and the antiviral effect on virus infection was tested. His-SPOCK2 proteins were purified separately from the total cell lysate or from the cultured medium of His-SPOCK2-transfected CHO cells using nickel-nitrilotriacetic acid (Ni-NTA) resin. In contrast to intracellular SPOCK2 (approximately 70 kDa) prepared in cell lysates, SPOCK2 from the culture medium was heavily glycosylated (Fig. 3E). Furthermore, purified SPOCK2 from the culture medium was more effective than SPOCK2 from the cell lysates (Fig. 3F). Based on this experimental evidence, we concluded that SPOCK2 is secreted into the extracellular space in a highly glycosylated and active form.

To evaluate the antiviral effect of SPOCK *in vivo*, sublethal doses of influenza A virus (IAV) PR8 strains mixed with dialysis buffer or purified SPOCK2 proteins (10 μg) were intranasally administered, and the condition of the infected mice was monitored for up to 3 weeks postinfection. Every mouse in the control group experienced severe weight loss after infection and then recovered. In contrast, SPOCK2-treated mice appeared healthy (Fig. 3G). Signs of lung inflammation were evident in the control group of mice: expanded bronchiolar walls, disorganized alveolar structure, and the infiltration of inflammatory immune cells. In contrast, the alveolar structure of the SPOCK2-cotreated mice was apparently normal, and the alveolar cavity was clean (Fig. 3H). Compared to the control mice, the SPOCK2-treated mice exhibited very low residual levels of virus infection in the lung (Fig. 3I and J). These results together suggest that extracellular SPOCK2 protects the host against virus infection.

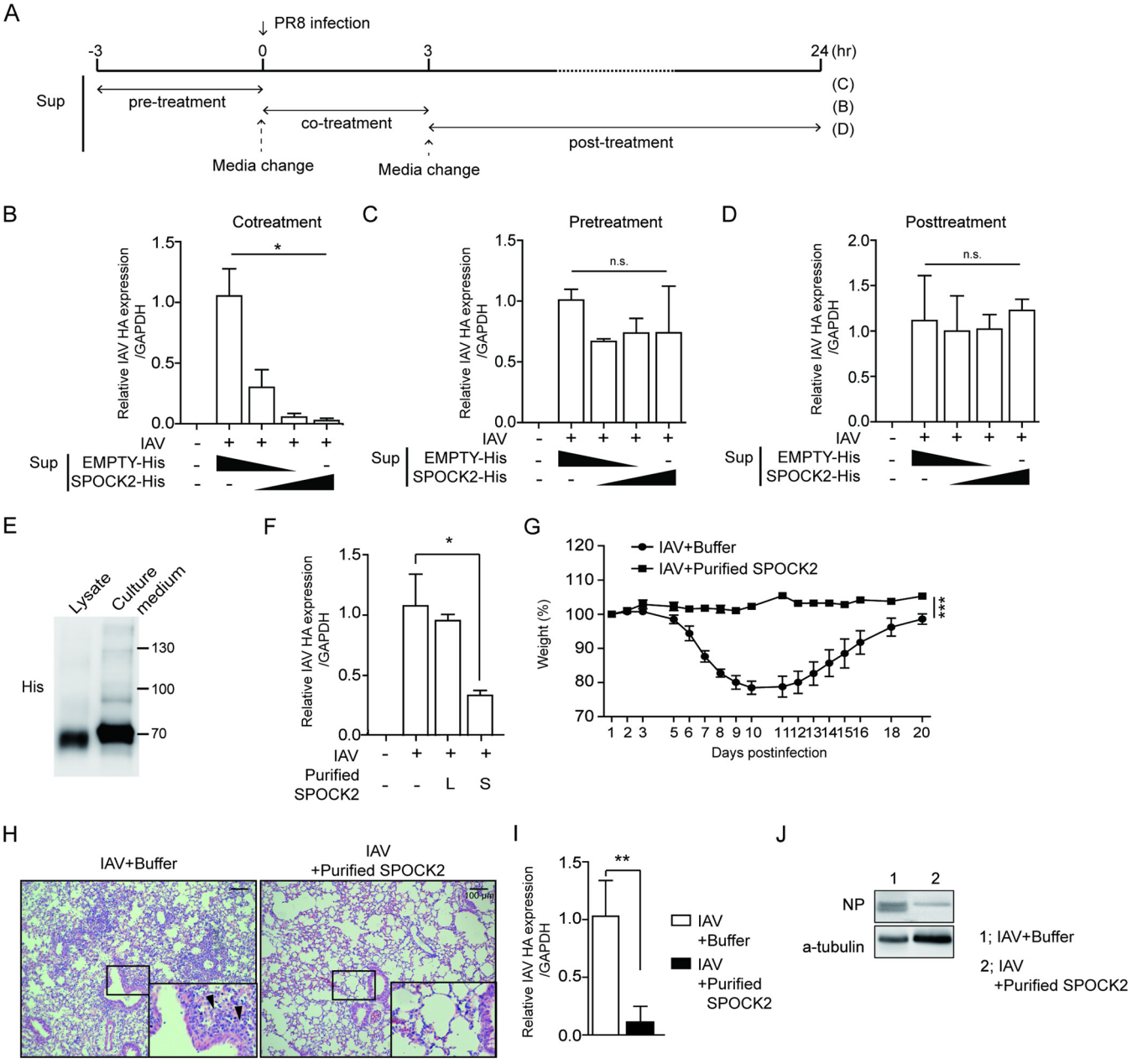

FIG 3 Recombinant SPOCK-2 protein inhibits virus infection *in vitro* and *in vivo*. (A) Schema of the experimental procedure. (B to D) A549 cells were infected with PR8 IAV (MOI, 0.1) in the presence of medium from SPOCK2-overexpressing cells. After 12 h, the cells under the indicated conditions were collected and HA vRNA expression was detected by qRT-PCR. Each bar indicates the average value ± SD obtained from triplicate experiments. *, $P < 0.05$; **, $P < 0.01$. (E) Purified SPOCK2 from lysate or culture medium was immunoblotted with anti-His. (F) A549 cells were infected with PR8 IAV (MOI, 0.1) in the presence of purified SPOCK2 (20 μg) from the lysate or medium of His-tagged SPOCK-overexpressing A549 cells. After 12 h, the cells under the indicated conditions were collected, and HA vRNA expression was detected by qRT-PCR. Each bar indicates the average value ± SD obtained from triplicate experiments. *, $P < 0.05$; **, $P < 0.01$ (*t* test). (G to J) Mice were intranasally infected with PR8 IAV at 50 PFU and treated with buffer or purified SPOCK2 at 10 μg per mouse. (G) Body weight changes in PR8 IAV virus-infected mice treated with buffer or purified SPOCK2 were monitored. The graph presents the average values ± SDs ($n = 6$ for each group). (H) Representative hematoxylin and eosin (H&E) histology of lung tissues from the three mice in panel G evaluated at 7 days postinfection (dpi). The enlarged image shows the bronchiole region. Arrows indicate infiltration of inflammatory cells. (I) The intracellular copy numbers of the PR8 IAV HA gene and IFN-β in lung tissues at 7 dpi from the mice in panel G were measured by qRT-PCR. Each bar indicates the average value ± SD ($n = 3$). (J) The intracellular amount of the PR8 IAV NP gene in lung tissues at 7 dpi from the mice in panel G were measured by immunoblotting ($n = 3$). *P* values were calculated by two-way ANOVA. **, $P < 0.01$; ***, $P < 0.001$.

The heparan sulfate moiety of the SPOCK2 proteoglycan is important for antiviral activity. The core protein of SPOCK2 consists of multiple distinct domains, including a signal peptide in the amino terminus, a cysteine-rich domain homologous to the follistatin (FS) domain, an extracellular calcium-binding (EC) domain that harbors

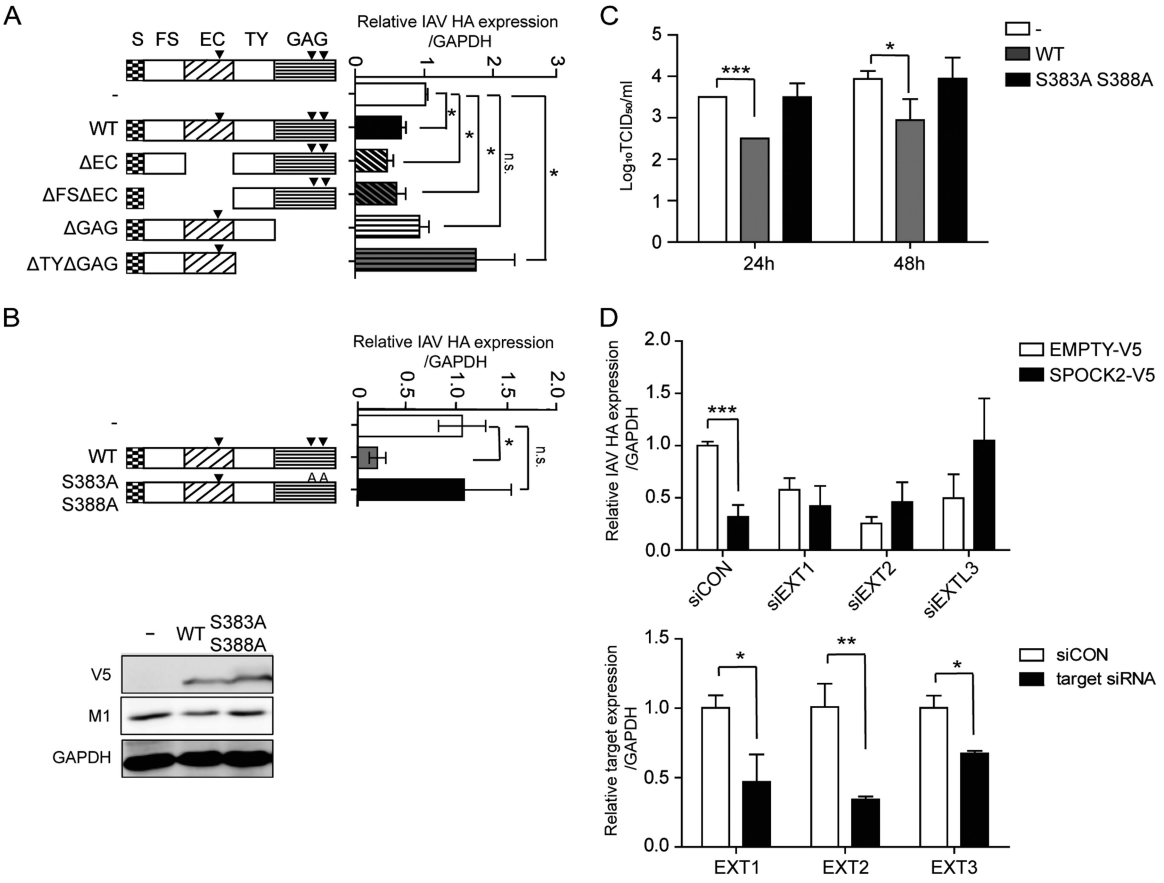

FIG 4 The heparan sulfate moiety is responsible for the antiviral effect of SPOCK2. (A) Domain deletion mutants of SPOCK2 were overexpressed in A549 cells and infected with PR8 IAV for 24 h. HA vRNA levels were measured by qRT-PCR. (B) Site-directed mutants of SPOCK2 were overexpressed in A549 cells and infected with PR8 IAV for 24 h. HA vRNA levels were measured by qRT-PCR. For the bottom portion, cell lysates from the top portion were analyzed with anti-M1 and anti-V5, and anti-GAPDH was detected as a loading control. (C) At 36 h posttransfection, A549 cells were infected with IAV at an MOI of 1 per well for 24 h or 48 h. The supernatants from cells infected with A549 cells were collected, and the viral titers were measured by the $TCID_{50}$ method. The bars indicate the mean values ± SDs obtained from three experiments. (D) A549 cells were transfected with EXT1, -2, and -3 siRNAs and a V5-tagged SPOCK2-expressing construct or empty vector. HA vRNA levels were measured by qRT-PCR. The expression was normalized by GAPDH (upper graph). The silencing efficiencies of EXT1, EXT2, and EXTL3 were measured by qRT-PCR (lower graph). Expression was normalized by GAPDH. All graphs indicate the average values ± SDs obtained from triplicate experiments. ***, $P < 0.001$ (*t* test).

an N-glycosylation site, thyroglobulin (TY) domains with a CWCV motif, and a carboxyl region with two GAG-binding motifs (GAG domain). To characterize the domain of SPOCK2 responsible for the regulation of antiviral activity, various deletion constructs were generated, including a construct without the EC domain (ΔEC) and a construct without the GAG domain (ΔGAG) (Fig. 4A). Each construct was transiently transfected, and the intracellular amounts of influenza virus after infection were measured. The antiviral activity of deletion mutants that lacked the EC domain alone or lacked both the EC and FS domains was as effective as that of wild-type (WT) SPOCK2. In contrast, the antiviral activity of SPOCK2 disappeared when either the SPOCK2 (ΔGAG) or SPOCK2 (ΔTY ΔGAG) mutant was overexpressed, suggesting that the antiviral activity of SPOCK2 is derived from the protein regions containing the GAG domain or from the GAG chains attached to this domain. These results suggest that the antiviral activity of SPOCK2 depends on the attached GAG motif. Unexpectedly, those SPOCK2 mutants without TY and GAG domains exhibited somewhat proviral activity, with higher levels of intracellular virus accumulation than the control. Although there is no report about the TY domain in SPOCK2, the purified TY domains of SPOCK1 and -3 are reported to act as inhibitors of cathepsin L and B, respectively (20–22). Cathepsin is known to function during influenza virus infection; therefore, it is also possible that SPOCK2

performs an additional regulatory role during infection by interaction of cathepsin with the TY domain. To verify importance of the GAG motif for the antiviral activity of SPOCK2, double point mutations were introduced at the S383 and S388 residues, where the heparan sulfate GAG chains are attached. The overexpressed SPOCK2 (S383A S388A) mutant did not exert antiviral activity, as measured by the intracellular viral HA expression and the $TCID_{50}$ per milliliter of influenza virus (Fig. 4B and C).

To determine whether the heparan sulfate chains that attach to SPOCK2 are indeed critical for inhibiting virus infection, the expression of the exostosins EXT1, EXT2, and EXTL3 was silenced and the antiviral effect of SPOCK2 was assessed. Exostosins have glycosyltransferase activities for heparan sulfate biosynthesis. In exostosin-silenced cells, GlcNAc and GlcA transferase activities are decreased, resulting in the production of shorter heparan sulfate chains (23–25). In EXT1-, EXT2-, or EXTL3-silenced cells, the antiviral effect of SPOCK2 significantly disappeared, confirming that the heparan sulfate chains of SPOCK2 are necessary for its antiviral effects against influenza virus infection (Fig. 4D).

SPOCK2 blocks the attachment and entry of influenza virus. The ECM is a noncellular structure composed of various proteoglycans and glycoproteins. Viruses use proteoglycans to facilitate cell attachment and internalization into host cells (26). Since SPOCK2 is a secreted form of proteoglycan with heparan sulfate chains, we wondered whether SPOCK2 functions to block the attachment and entry of the virus. Using the purified His-SPOCK2 protein and 1,1′-dioctadecyl-3,3,3′,3′-tetramethylindocarbocyanine perchlorate (DiI)-labeled virus, we therefore examined the inhibitory effect of His-SPOCK2 on viral entry. At 20 min postinfection, DiI was detected in the cytoplasm of the control cells. In contrast, a very low DiI signal appeared in the cytoplasm of the purified SPOCK2-treated cells (Fig. 5A). We also separately assessed internalized vRNA 20 min after virus infection in the absence or presence of SPOCK2 treatment. A smaller amount of vRNA was detected when purified SPOCK2 was used in the treatment (Fig. 5B). These studies suggest that purified SPOCK2 might act on the extracellular compartment to inhibit viral entry. To investigate whether SPOCK2 could directly interfere with viral attachment, we next performed a hemagglutination inhibition (HI) assay, which measures the ability of the virus to attach to receptors on red blood cells (RBCs). A serially diluted influenza virus was incubated with the same concentration of RBCs, and the virus titer distinguishing agglutinated and nonagglutinated (suspended) cells was monitored. When purified SPOCK2 was included in the reaction, viral attachment to RBCs was suppressed in a dose-dependent manner (Fig. 5C). This finding suggests that purified SPOCK2 inhibits influenza virus at the attachment stage. The antiviral activities of purified SPOCK2 were further examined with a plaque assay. The number of plaques produced was then recorded and analyzed as percentage of untreated virions. Cotreatment with the purified SPOCK2 (20 μg) reduced the number of plaques, indicating that SPOCK2 efficiently inhibits influenza virus plaque formation (Fig. 5D).

We also examined the effect of SPOCK2 on influenza virus replication. To this end, we established an assay to measure RNA-dependent RNA polymerase activity. We transfected an enhanced green fluorescent protein (eGFP) reporter plasmid carrying NS vRNA along with a plasmid expressing PB1/PB2/PA with or without NP. The viral RNA-dependent RNA polymerase (RdRp) activity was assessed by measuring the mean fluorescence intensity of GFP. The results indicated that all four constructs were necessary to express GFP (Fig. 5E). Next, we investigated the effect of SPOCK2 on RdRp activity. However, the alteration of SPOCK2 levels did not affect the activity of influenza virus RdRP, indicating that the SPOCK2 protein most likely functions during the internalization of virus particles but not during viral genome replication (Fig. 5F).

The sialic acid moiety of SPOCK2 protein is used for binding to influenza virus. SPOCK2 is a heavily glycosylated proteoglycan with two different types of attached glycosylated moieties: the N-glycosylated moiety on the EC domain and the heparan sulfate chains on the GAG domains. We speculate that the molecular weight of the endogenous SPOCK2 core protein is approximately 55 kDa, based on the electrophoretic mobility shift after tunicamycin treatment (Fig. 6A). Tunicamycin inhibits the

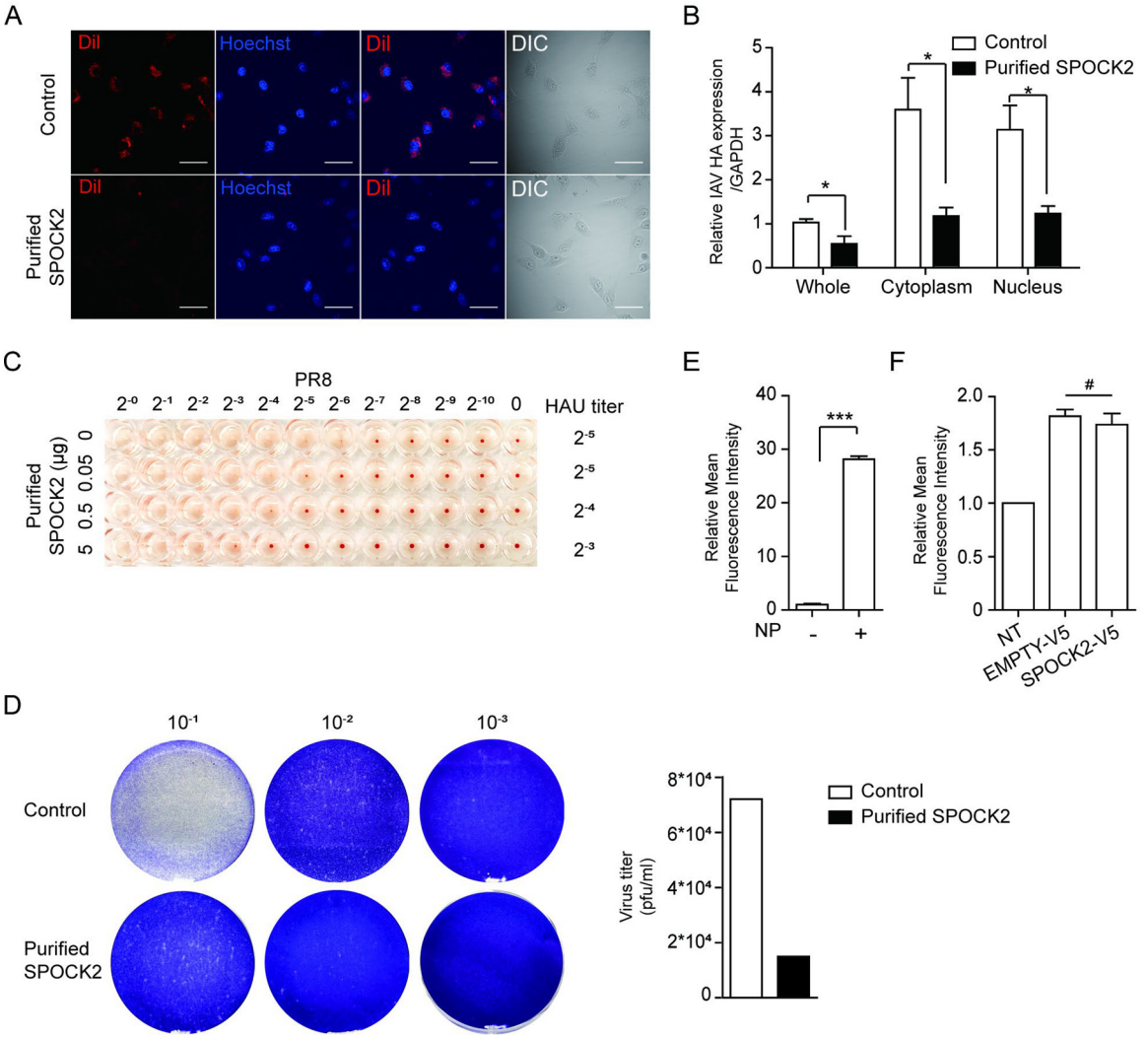

FIG 5 Purified SPOCK2 inhibits attachment and entry of influenza virus. (A) A549 cells were infected with DiI-labeled PR8 IAV with buffer or 20 μg of purified SPOCK2 for 20 min. DiI and nucleus (Hoechst) staining were examined by confocal microscopy. Representative images are shown. Scale bars, 200 μm. DIC, differential interference contrast. (B) A549 cells were infected with PR8 IAV in the presence of purified SPOCK2 (20 μg) for 20 min and then processed for subcellular fractionation. The fractions from different compartments were used for RNA isolation and the determination of HA vRNA levels by qRT-PCR. Each bar indicates the average value ± SD obtained from triplicate experiments. *P* values were calculated by two-way ANOVA. *, $P < 0.05$. (C) An HI assay was performed using turkey RBCs. The RBCs were added to a 96-well v-bottom plate. PR8 IAV was added with serially diluted purified SPOCK2 and incubated for 1 h at room temperature. The inhibition of PR8 IAV attachment to RBCs was then measured by observing each well. (D) Plaque assays of PR8 IAV with buffer or purified SPOCK2 (20 μg). (E) HEK293T cells were transfected with PB1, PB2, PA, and eGFP plasmid carrying NS1 vRNA with or without NP plasmid. After 48 h, the relative mean fluorescence intensity of GFP was measured by FACS. All graphs indicate the average values ± SDs obtained from triplicate experiments. ***, $P < 0.001$. (F) A549 cells were transfected with NP, PB1, PB2, PA, an eGFP plasmid carrying NS1 vRNA and a V5-tagged SPOCK2 expression construct or empty vector. After 48 h, the mean fluorescence intensity of GFP was measured by FACS. NT, transfection of reporter segment alone. Each bar indicates the average value ± SD obtained from triplicate experiments. #, $P > 0.05$ (not significant).

formation of N-glycosidic linkages during the early steps of glycoprotein synthesis in the Golgi, thereby blocking glycosylation at an early step. In contrast, the molecular weight of endogenous SPOCK2 shifted from approximately 100 kDa to 70 kDa when cell lysates were treated with peptide-*N*-glycosidase F (PNGase F), which cleaves N-linked oligosaccharides (Fig. 6B). We observed previously that the molecular weight of endogenous SPOCK2 decreased upon virus infection but not after IFN or poly(I·C) treatment (Fig. 1C, D, and G). This observation led us to hypothesize that influenza virus possesses activity that cleaves the core protein or oligosaccharide portions of SPOCK2. We first examined the effect of the neuraminidase (NA) protein of influenza virus on SPOCK2 because NA has intrinsic neuraminidase activity that cleaves sialic acid (SA) and an adjacent

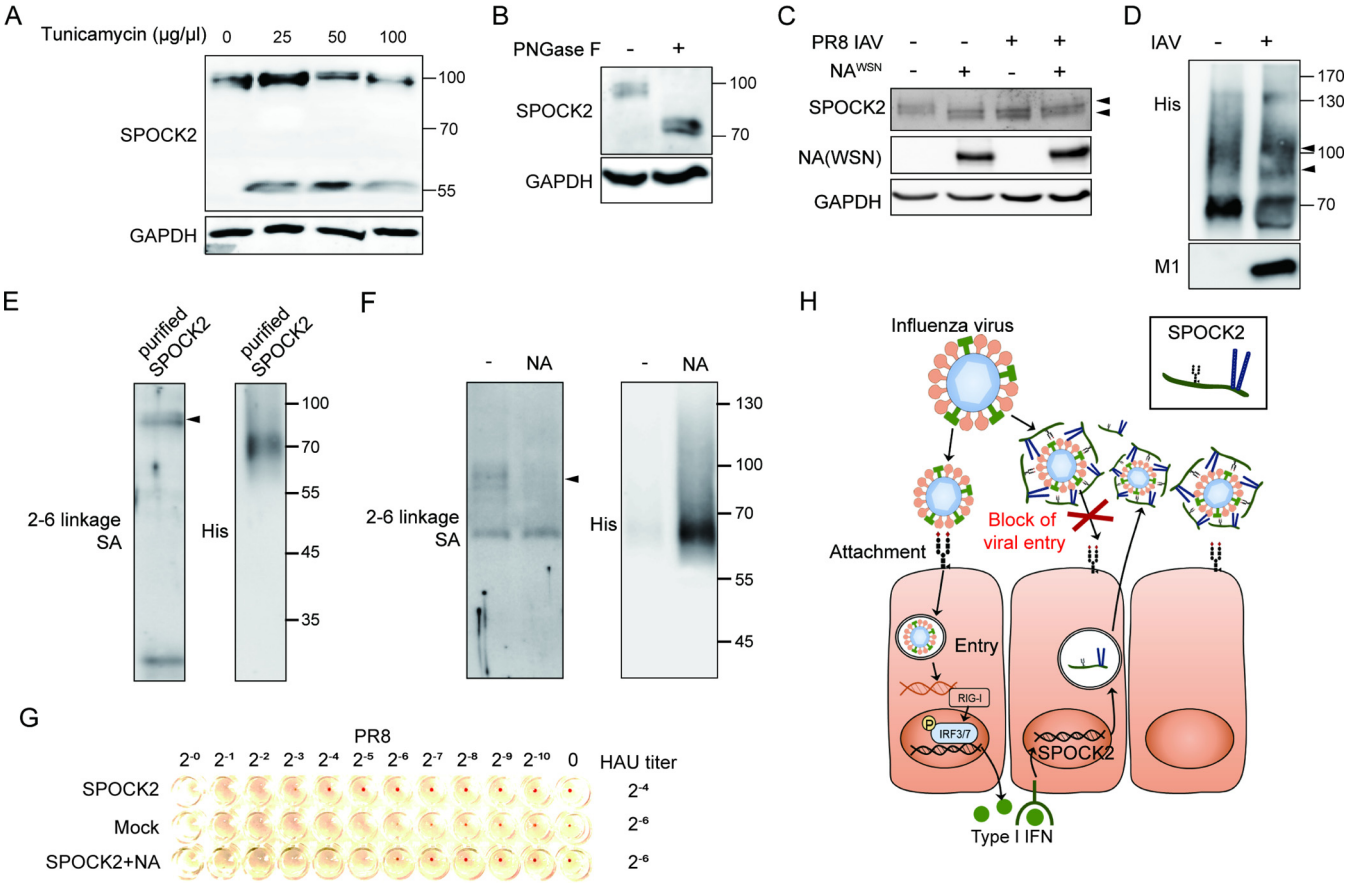

FIG 6 Influenza virus preferentially binds the sialic acid moiety of SPOCK2. (A and B) A549 cells treated with tunicamycin for 12 h (A) or PNGase F (250 U) (B) were subjected to immunoblot analysis with anti-SPOCK2, and anti-GAPDH was detected as a loading control. (C) Lysates of empty vector- or NA-expressing A549 cells infected with PR8 IAV for 12 h were subjected to immunoblot analysis with anti-SPOCK2 and anti-NA. Anti-GAPDH was detected as a loading control. (D) Purified SPOCK2 (1 μg) was incubated with PBS or PR8 IAV for 1 h and subjected to immunoblot analysis with anti-His and anti-M1. (E and F) Purified SPOCK2 (1 μg) from SPOCK2-overexpressing cells (E) or NA-co-overexpressing cells (F) analyzed by Western blotting and SNA blotting. (G) An HI assay was performed using turkey RBCs. The RBCs were added to a 96-well v-bottom plate. PR8 IAV was added with serially diluted purified SPOCK2 from the medium of SPOCK2-overexpressing cells or NA-co-overexpressing cells and incubated for 1 h at room temperature. The inhibition of PR8 IAV attachment to RBCs was then measured by observing each well. (H) Schematic illustration of the proposed model.

sugar residue. NA protein from the influenza virus WSN strain was transiently transfected, and changes in the molecular weight of endogenous SPOCK2 protein were observed. NA overexpression alone was sufficient to alter the size of the SPOCK2 protein to a degree equivalent to that observed with influenza virus infection (Fig. 6C). Differences in molecular weight similar to those described above were observed using purified SPOCK2 *in vitro* (Fig. 6D). The results indicate that SPOCK2 might possess a sialic acid moiety.

To verify the presence of a sialic acid moiety on SPOCK2, purified SPOCK2 was analyzed by using biotinylated *Sambucus nigra* lectin (SNA), which binds to 2,6-linkage-specific sialic acid (Fig. 6E). Typically, most proteoglycans appear as smear bands when separated by SDS-PAGE because of the heterogeneity of the carbohydrate portion. The main portions of purified SPOCK2 migrate approximately at the 70-kDa position, with long smear bands higher than 70 kDa. In contrast, lectin is specific to 2,6-linkage sialic acid, meaning that it detects only SPOCK2 with 2,6-linkage SA attachment. Our data indicate that SPOCK2 with the sialic acid moiety migrates at approximately 100 kDa, indicating that it is highly glycosylated form. It is known that the influenza virus HA protein binds to receptor proteins that carry sialic acid to initialize attachment and entry. NA cleaves sialic acid from viral receptors to allow viral release. Therefore, we hypothesized that the reduction in the size of SPOCK2 observed upon virus infection or NA overexpression could be due to viral NA cleavage of the sialic acid moiety of SPOCK2. In support of this hypothesis, the 2,6-linkage sialic acid moiety was not

detected in the SPOCK2 purified from NA-co-overexpressing cells (Fig. 6F). To evaluate whether the sialic acid moiety of SPOCK2 is needed for antiviral activity, the HI assay was performed with SPOCK2 protein purified from cells expressing SPOCK2 alone or from cells co-overexpressing SPOCK2 and NA (Fig. 6G). The inhibitory effect of SPOCK2 on viral attachment to RBCs disappeared when equal amounts of SPOCK2 protein purified from the NA-coexpressing cells were used, indicating that SPOCK2 inhibits influenza virus attachment to its receptors and that its sialic acid moiety is required for this activity. In addition, NA can cleave the sialic acid moiety of SPOCK2, thereby evading the antiviral activity of SPOCK2.

DISCUSSION

In this paper, we report a novel IFN-inducible heparan sulfate proteoglycan (HSPG), SPOCK2, that inhibits the attachment to and entry of influenza virus into cells. SPOCK2 expression was induced in the lung upon virus infection and in AECs upon treatment with type I IFN, IFN-α. The core protein of SPOCK2 possesses multiple target sites for glycosylation that work in different ways to control virus infection. An N-glycan chain attached to Asn252 in the EC domain of SPOCK2 has a 2,6-linked sialic acid moiety, which acts as a binding receptor for influenza virus. In contrast, heparan sulfate glycans covalently attached to Ser383 and Ser388 in the C-terminal domain of SPOCK2 were essential for the antiviral activity of SPOCK2, which blocks viral entry. In this report, we demonstrate that SPOCK2 inhibits viral invasion using the heparan sulfate chain of proteoglycans. At the same time, we demonstrate that viral HA attachment to the host utilizes the sialic moiety of SPOCK2, while NA cleaves the sialic acid moiety of SPOCK2, resulting in inhibition of SPOCK2 activity. Based on the observation that SPOCK2 is a secreted HSPG and that its protein level is increased during infection, we propose that SPOCK2 is an IFN-inducible decoy receptor that competes with the cell surface receptor for influenza virus (Fig. 6H).

Proteoglycans are complex macromolecules with multiple glycan chains attached to core proteins and are mainly localized on the cell surface or in the ECM. Proteoglycans are composed of components of the matrix compartment and actively participate in various biological responses through the regulation of signaling pathways. The regulatory roles of proteoglycans in tissue homeostasis and pathological transition during development, wound healing, and inflammation have been actively studied (27). Heparan sulfate, one of the most frequently observed glycans, is reported to be a receptor for various cytokines, chemokines, and growth factors. The heparan sulfate chain of CD44 acts as a CD11b/CD18 counterreceptor that results in the inhibition of inflammation (28).

The abundant heparan sulfate works as a platform to capture enteric viruses (e.g., rotavirus and norovirus) and facilitate viral attachment and internalization into host cells (26). Proteoglycans can be released to the cell surface or extracellular matrix through the canonical secretion pathway or proteolytic cleavage. The most soluble form of the cell surface receptor should bind to the virus and, in turn, inhibit the binding of the virus to receptor-bearing cells. For example, soluble heparin can bind to the HSV virion, resulting in the inhibition of binding to host cells (29). No direct relationship between influenza virus invasion and proteoglycans has been reported. However, a proteoglycan, syndecan-1, is reported to have the ability to suppress influenza virus infection (30). Moreover, the amount of heparan sulfate correlates with the internalization of human parainfluenza virus type 3 (HPIV-3). Although HPIV-3 is internalized using sialic acid receptor, a previous paper (31) suggested that the internalization of HPIV-3 is reduced by preincubation with the soluble form of heparan sulfate. This finding indicates that the soluble form of heparan sulfate can inhibit virus infection by utilizing sialic acid internalization, as SPOCK2 does.

The respiratory tract is a major site of entry for viruses, but a multilayered antiviral fence protects the host against infection (32). The lung epithelial layers are positioned at the outermost region of the lung and create a physical barrier against virus infection. Upon infection, the lung epithelium also expresses various inflammatory molecules and immune defense proteins. Alveolar type II (ATII) respiratory epithelial cells are central to

the lung defense and are also a site of influenza A virus infection. The physiological role of SPOCK2 has been recently proposed to relate to the lung, based on the finding of its genetic linkage to bronchopulmonary dysplasia and alveolarization (6). SPOCK2 mRNA expression was detected in lung fibroblasts and AECs during lung development and after tissue injury induced by treatment with environmental stressors, such as hyperoxia or perfluoroalkyl substances (33). In addition, SPOCK2 expression has been reported to increase during the transitioning of type II epithelial cells to type I epithelial cells (34). In this study, we observed increased SPOCK2 expression during virus infection in A549 cells and in mouse lungs. Moreover, cells directly treated with purified SPOCK2 or with medium from SPOCK2-overexpressing cells were efficiently protected against influenza virus infection at early stages of infection. Based on these observations, we propose SPOCK2 as an extracellular component of the lung that functions as a barrier against infection. However, a number of sialoglycosylated proteins and other sialoglycans can also neutralize influenza virus virions in the extracellular compartment. For the model we propose to be relevant, the total levels of extracellular sialoglycans should be increased significantly as a result of the increased release of SPOCK2, or SPOCK2 must have a much higher affinity or avidity for the virions than the other available glycans. Further investigations demonstrating the detailed regulatory mechanism of SPOCK2 inhibition of influenza virus in the extracellular matrix are needed.

Influenza virus infection is initiated by the binding of HA to the sialylated moiety of the cell surface receptor on respiratory epithelial cells. Internalization of the receptor-bound influenza virus is followed by clathrin-mediated endocytosis. Because SPOCK2 is a secreted HSPG with a sialylated moiety on its N-glycan chain, it is highly likely that SPOCK2 binds directly to influenza virus in the extracellular compartment to block viral attachment to the cell surface receptor. Although we have not experimentally shown other mechanisms, there are other possible ways that SPOCK2 might intervene during the internalization step of influenza virus infection. Ca^{2+} activity or Ca^{2+}-mediated signaling pathways are necessary to mediate the clathrin-mediated endocytosis of influenza virus. The calcium level in the ECM affects the infectivity of influenza virus (35, 36). Notably, SPOCK2 possesses an EC domain, which is reported to have calcium-binding ability (37). Therefore, it will be of interest to further investigate the regulation of SPOCK2 activity depending on the local calcium concentration and examine the potential to control influenza virus infection.

Here we present a new class of ISGs that work against virus infection. Most known ISGs that target the virus itself usually function to block viral replication or to inactivate viral proteins inside infected host cells (38–41). For example, MxA inhibits viral replication by interacting directly with the viral proteins NP and PB2. IFITM3 blocks the entry of influenza virus by promoting the degradation of virions after internalization (42, 43). In contrast, SPOCK2 works outside the cell during the very early steps of viral attachment to the host cell surface. Because the site of antiviral action is the extracellular compartment and because it has shown efficacy in treatment prior to virus infection, SPOCK2 is an attractive target for preventive vaccine development. More intensive research to engineer and enhance the antiviral efficacy of SPOCK2 is thus needed.

MATERIALS AND METHODS

Ethics statement. The production and infection of A/Puerto Rico/8/34 (PR8) IAVs was performed in compliance with the guidelines established by the Genetic Recombination Experiment Policy of the Institutional Biosafety Committee (IBC) at Pohang University of Science and Technology (POSTECH) under approval number PIBC-016. Mouse experimental procedures were approved by the Institutional Animal Care and Use Committee (IACUC) at POSTECH under the standard IACUC guidelines (registration number 11-1543061-000268-14) of the Animal and Plant Quarantine Agency (APQA) and Ministry of Food and Drug Safety (MFDS) of Korea with permit number POSTECH-2018-0017 (experimental influenza infection). All mouse experiments were performed in a biosafety level 2 facility that was accredited by the Korea Centers for Disease Control & Prevention (KCDC). For the data presented, 18 mice were used, of which 6 were euthanized at the end of the experiment and 12 were euthanized in anticipation of reaching the human endpoint. No mice died at other points in the experiment.

Cells and reagents. Human embryonic kidney 293T (HEK293T) (obtained from the ATCC, Manassas, VA), human lung epithelial A549 (obtained from the ATCC), Chinese hamster ovary CD44 (CHO DG44) (kind gift from Jeong-Hoe Kim, KAIST, Daejeon, Republic of Korea), and HeLa (obtained from the ATCC)

were used. A549, HEK293T, CHO DG44, and HeLa cells were grown in Dulbecco's modified Eagle's medium (DMEM; Serena). The cell culture medium was supplemented with 10% fetal bovine serum (FBS; HyClone, Logan, UT) and 1% penicillin-streptomycin (Invitrogen, Carlsbad, CA). Cells were incubated at 37°C and 5% CO_2. For stimulation, the cells were treated with IL-1β (R&D Systems, Minneapolis, MN), IL-6 (R&D Systems), tumor necrosis factor alpha (R&D Systems), transforming growth factor β (TGF-β; R&D Systems), IFN-α (R&D Systems), and IFN-β (R&D Systems). Cells were treated with cytokines at the desired concentrations in DMEM (with 10% FBS) for the desired times. To inhibit N-linked glycosylation, A549 cells were incubated with tunicamycin (Calbiochem) in a dose-dependent manner (0, 25, 50, and 100 μg), or lysate from A549 cells was incubated with PNGase F (New England BioLabs [NEB]).

Virus purification and titration. Human PR8 was originally provided by Adolfo Garcia-Sastre. Virus was grown in 14-day-old embryonated eggs, and allantoic fluid was collected. Fluids were subjected to sucrose gradient centrifugation in an SW28 rotor (Beckman) at 125,000 $\times$ *g* for 1 h at 4°C. The virus bands appeared at the interface between 30% and 60% sucrose. The virus particles were subsequently pelleted by centrifugation at 125,000 $\times$ *g* for 1 h at 4°C. The virion pellets were resuspended in 200 μl of 1% bovine serum albumin (BSA) in Opti-MEM. A549 cells were seeded in 24-well plates 12 h prior to virus infection. The virus was 10-fold serially diluted with medium and added to each well with three technical replicates for each dilution. After 1 h of incubation, the supernatants were removed, and fresh growth medium containing 1% FBS was added. After 72 h, the cells were fixed with 4% paraformaldehyde and stained with crystal violet. Subsequently, the $TCID_{50}$ was calculated. To estimate the effect of SPOCK2 on the virus titer, SPOCK2-overexpressing or SPOCK2-silenced A549 cells were infected with PR8 at a multiplicity of infection (MOI) of 1. The supernatant and cell were collected at 24 or 48 h postinfection. The virus titer was determined in A549 cells as described above.

IAV infection in cells. For general infection, cells were incubated with virus in serum-free DMEM for 1 h, washed with phosphate-buffered saline (PBS), and further incubated in DMEM (with 10% FBS) until the desired time was reached (including the initial incubation time).

For pretreatment, we changed the medium from normal growth medium to SPOCK2-containing medium prior to infection. At 3 h postinfection, we changed the medium from SPOCK2-containing medium to normal growth medium. In the case of cotreatment, the virus was preincubated in SPOCK2-containing medium and then applied to the cells. After 3 h, we changed to normal growth medium. For posttreatment, the virus was applied to the cells first to allow infection, and 3 h later, the medium was changed to purified SPOCK2-containing medium. In all infection experiments, we administered the virus after washing the cells with PBS.

IAV infection in mice. Nine-week-old female BALB/c mice were intranasally inoculated with 50 PFU of IAV PR8, in a total volume of 50 μl, and monitored for survival and weight loss for 21 days. The PR8 stock aliquot was thawed and diluted in saline before use. For treatment with purified SPOCK2, PR8 was mixed with buffer or purified SPOCK2 to adjust the total volume to 50 μl and then administered intranasally to the mice.

Virus fluorescence labeling. DiI is a lipophilic dye that integrates into the virion without changing the biophysical properties of the virus. PR8 influenza virus was incubated with DiI (Thermo Fisher) solution for 1 h at room temperature. The virus in fluorescent label solution was applied to a spin column containing Sephadex G50 beads (Pharmacia, USA) and centrifuged for 2 min at 4,000 rpm to remove excess unbound fluorescent label dye. The flowthrough fraction was used for the manipulation of a single virus. DiI-labeled influenza virus was applied to A549 cells for the attachment and entry assay.

Plaque assay. Monolayered HeLa cells were infected with 10-fold serially diluted IAV PR8 allantoic fluids mixed with dialysis buffer or purified SPOCK2 proteins (20 μg) for 30 min. The cells were washed with PBS and overlaid with the medium (50% 2$\times$ DMEM, 50% gum tragacanth, and 5% FBS). After 72 h, the cells were fixed with 4% paraformaldehyde and stained with crystal violet. Subsequently, the plaques were counted to determine viral titers.

Expression and purification of human SPOCK2 protein. A DNA fragment encoding human SPOCK2 (1 to 425 amino acids) was subcloned into an expression vector derived from the pDEST-V5 plasmid. The vector was designed to express SPOCK2 as a fusion protein containing 6$\times$ His as the after-signal peptide. This 6$\times$ His-containing human SPOCK2 expression plasmid was transfected into mammalian cells (HEK293T or CHO DG44) with polyethylenimine (PEI; Polysciences). To purify the secreted His SPOCK2 protein, the medium was harvested from the transfected cells by pelleting the cells by centrifugation (1,500 rpm, 2 min, and 4°C). The medium was supplemented with 2 mM β-mercaptoethanol (Sigma) and phenylmethylsulfonyl fluoride (PMSF) and incubated with Ni-NTA beads (Qiagen) for 2 h. After 2 rounds of washing with wash buffer (50 mM NaH_2PO_4, 300 mM NaCl, 20 mM imidazole, 2 mM β-mercaptoethanol [pH 8.0]), Ni-NTA beads were loaded into Poly-Prep chromatography columns (Bio-Rad). After 4 rounds of washing with wash buffer, human His-SPOCK2 protein was eluted with elution buffer (50 mM NaH_2PO_4, 300 mM NaCl, 250 mM imidazole, 2 mM β-mercaptoethanol [pH 8.0]). To remove the imidazole, two rounds of dialysis were conducted with dialysis buffer (50 mM NaH_2PO_4, 300 mM NaCl, 2 mM β-mercaptoethanol [pH 8.0]). Dialyzed His-SPOCK2 was concentrated with Amicon Ultra-15 centrifugal filters (NMWL 3K; Millipore) by centrifugation (3,000 rpm and 4°C). After centrifugation, concentrated recombinant His-SPOCK2 was collected, and filtrated dialysis buffer was used as control buffer. Finally, recombinant human His-SPOCK2 protein was stored at 4°C.

RNA extraction and real-time RT-PCR. Total RNA was extracted using RNAiso Plus (TaKaRa), and 1 μg of total RNA was reverse transcribed using the Improm-II reverse transcription system (Promega). To detect influenza virus RNA, random oligomers were used for reverse transcription. To detect mRNA, oligo(dT) was used for reverse transcription. For PCR, SYBR premix *Ex Taq* (TaKaRa) was used, and threshold cycle (ΔC_T) values were obtained using the One-step real-time PCR system (Applied Biosys-

tems). The data were normalized against glyceraldehyde-3-phosphate dehydrogenase (GAPDH). The following primers were used: HA, 5′-TTGCTAAAACCCGGAGACAC-3′ and 5′-CCTGACGTATTTTGGGCACT-3′; IFN-β, 5′-TGCTCTCCTGTTGTGCTTCTCC-3′ and 5′-CATCTCATAGATGGTCAATGCGG-3′; SPOCK2, 5′-GCTGCGACGAGGATGGCT-3′ and 5′-CTACCAGATGTAGCCCCCGT-3′; GAPDH, 5′-GTGAAGGTCGGAGTCAACGG-3′ and 5′-CCACCCTGTTGCTGTAGCAGCCA-3′; EXT1, 5′-CTCTTGTCTCGCCCTTTTGT-3′ and 5′-TGGTGCAAGCCATTCCTACC-3′; EXT2, 5′-AAGCACCAGGTCTTCGATTACC-3′ and 5′-GAAGTACGCTTCCCAGAACCA-3′; EXTL3, 5′-CGCTCATCGCCCACTATTACC-3′ and 5′-TGTTCAGCTCTTGGCGCT T-3′; and IFN-αR1, 5′-GAAACCACTGACTGTATATTGTGTGAAA-3′ and 5′-CAGCGTCACTAAAAACACTGCTTT-3′.

RNA interference. Cells were transfected with the indicated short interfering RNA (siRNA) for 48 h by using Lipofectamine 3000. The following sequences were used: siControl, 5′-UUCUCCGAACGUGUCACGU-3′; siSPOCK2, 5′-GCAAUUUCAUGGAGGACGA-3′; EXT1, 5′-GGAUCAUCCCAGGACAGGA-3′; EXT2-2, 5′-GGUGUAUAUCUAUGCUCUG-3′; EXT2-2, 5′-GGAGACAGCACAAGCGAUG-3′; EXTL3-1, 5′-GGCAGGCAAGCGGAUUUUU-3′; EXT3-2, 5′-GGUCUCUUCCUUACCCUUU-3′; and IFN-αR1, 5′- AACAGCCAUUGAAGAAUCUUCTT-3′.

Western blotting and immunofluorescence (IF) staining. For Western blot analysis, cells were lysed in lysis buffer (25 mM Tris [pH 7.5], 150 mM NaCl, 1% Triton X-100, 0.1% SDS, and 0.5% deoxycholate with protease inhibitors), and 30 mg of total cell lysate was separated on SDS-polyacrylamide gels. Proteins were transferred onto a nitrocellulose membrane and analyzed with antibodies (Abs) against SPOCK2 (Santa Cruz Biotechnology), V5 (Invitrogen), influenza A virus matrix protein antibody (Bio-Rad), and GAPDH (Chemicon). Horseradish peroxidase (HRP)-conjugated secondary antibodies were added, and immunoreactive signals were visualized using an LAS4000 luminescent image analyzer (Fujifilm).

The following primary antibodies were used at the dilutions listed in parentheses: SPOCK2/testican-2 (N-15) (Santa Cruz Biotechnology, sc-49538; WB, 1:1,000), V5 (Invitrogen; R960-25; WB, 1:5,000; IF, 1:1,000), influenza matrix protein antibody GA2B (Bio-Rad; MCA401; WB, 1:1,000), anti-influenza A virus nucleoprotein antibody (C43) (Abcam; ab128193; WB, 1:1,000), and GAPDH (Chemicon; MAB374; WB, 1:25,000). The following secondary antibodies were used for immunoblot analysis: goat anti-mouse HRP-conjugated IgG (Pierce; 1858413; 1:10,000), goat anti-rabbit HRP-conjugated IgG (Pierce; 1858415; 1:10,000), donkey anti-goat HRP-conjugated IgG (Santa Cruz Biotechnology; sc-2020; 1:5,000), and HRP-labeled streptavidin (Bioss, Beijing, China). For immunofluorescence staining, cells on coverslips were fixed with 4% paraformaldehyde. Slides were mounted and analyzed using an Olympus confocal microscope. The images were processed with ImageJ.

Lectin blot analysis. First, 1 μg of purified SPOCK2 was subjected to 10% SDS-PAGE and transferred. Then, 2 μg/ml of biotinylated *Sambucus nigra* lectin (SNA) (Vector Labs; B-1305), which specifically binds to sialic acid to terminal galactose via α2,6-linkages, was applied. HRP-labeled streptavidin (Pierce; 21126) was used for the recognition of biotinylated SNA.

HI assay. A 50-μl aliquot of 0.7% turkey RBCs was added to a 96-well v-bottom plate. For hemagglutination inhibition (HI) assays, influenza virus A/Puerto Rico/8/34 was added, and the virus was coincubated with serially diluted SPOCK2 for 1 h at room temperature. The hemagglutination patterns were read after 1 h of incubation. The dose at which aggregation occurred was determined.

Cell fractionation. Cells were washed with reticulocyte standard buffer (RSB; 10 mM Tris-HCl [pH 7.4], 10 mM NaCl, 3 mM $MgCl_2$), then incubated for 3 min on ice, pelleted at 7,000 rpm and 4°C for 3 min, and resuspended by slow pipetting with lysis buffer (RSB40; 10 mM Tris-HCl [pH 7.4], 10 mM NaCl, 3 mM $MgCl_2$, 10% glycerol, 0.5% NP-40, 0.5 mM dithiothreitol [DTT], 100 U/ml of rRNasin). The supernatant was designated the cytoplasmic fraction and centrifuged at 7,000 rpm and 4°C for 3 min. The pellet was designated the nuclear fraction. The cytoplasmic and nuclear fractions were suspended in RNAiso Plus (TaKaRa). "Whole-cell fraction" refers to RNA from whole cells without fractionation. Equal amounts (1 μg) of total RNA from the whole-cell, cytoplasmic, and nuclear fractions were analyzed.

Luciferase assay. A549 cells in 24-well plates were transfected with pSPOCK2-luc (700 ng) and pRL-TK (15 ng) for normalization of the transfection efficiency. The dual-luciferase assay was performed according to the manufacturer's instructions (Promega).

FACS analysis. To measure RdRp activity, cells were transfected with RdRp component (plasmid) and GFP-tagged NS1 antisense. After 48 h, cells were detached with trypsin and washed with PBS. The cells were washed with fluorescence-activated cell sorting (FACS) (1% FBS in PBS) buffer by centrifugation at 3,000 $\times$ *g* and 4°C for 5 min. Next, the cells were fixed with 4% paraformaldehyde in PBS. Fixed cells were washed with FACS buffer and analyzed with a flow cytometer (FACSCalibur; BD Biosciences, San Jose, CA).

ACKNOWLEDGMENTS

We thank Y. K. Choi for providing turkey RBCs.

This work was supported by a National Research Foundation of Korea (NRF) grant funded by the Korean government (Ministry of Science and ICT) (no. NRF-2015R1A2A1A10054957/2017R1A5A1015366).

We declare no competing financial interests.

REFERENCES

1. Stetson DB, Medzhitov R. 2006. Type I interferons in host defense. Immunity 25:373–381. https://doi.org/10.1016/j.immuni.2006.08.007.
2. Schoggins JW, Rice CM. 2011. Interferon-stimulated genes and their antiviral effector functions. Curr Opin Virol 1:519–525. https://doi.org/10.1016/j.coviro.2011.10.008.
3. Schneider WM, Chevillotte MD, Rice CM. 2014. Interferon-stimulated

genes: a complex web of host defenses. Annu Rev Immunol 32:513–545. https://doi.org/10.1146/annurev-immunol-032713-120231.
4. Liu J, Thorp SC. 2002. Cell surface heparan sulfate and its roles in assisting viral infections. Med Res Rev 22:1–25. https://doi.org/10.1002/med.1026.
5. Stencel-Baerenwald JE, Reiss K, Reiter DM, Stehle T, Dermody TS. 2014. The sweet spot: defining virus-sialic acid interactions. Nat Rev Microbiol 12:739–749. https://doi.org/10.1038/nrmicro3346.
6. Hadchouel A, Durrmeyer X, Bouzigon E, Incitti R, Huusko J, Jarreau PH, Lenclen R, Demenais F, Franco-Montoya ML, Layouni I, Patkai J, Bourbon J, Hallman M, Danan C, Delacourt C. 2011. Identification of SPOCK2 as a susceptibility gene for bronchopulmonary dysplasia. Am J Respir Crit Care Med 184:1164–1170. https://doi.org/10.1164/rccm.201103-0548OC.
7. Ito T, Couceiro JN, Kelm S, Baum LG, Krauss S, Castrucci MR, Donatelli I, Kida H, Paulson JC, Webster RG, Kawaoka Y. 1998. Molecular basis for the generation in pigs of influenza A viruses with pandemic potential. J Virol 72:7367–7373.
8. Ruoslahti E. 1988. Structure and biology of proteoglycans. Annu Rev Cell Biol 4:229–255. https://doi.org/10.1146/annurev.cb.04.110188.001305.
9. Gill S, Wight TN, Frevert CW. 2010. Proteoglycans: key regulators of pulmonary inflammation and the innate immune response to lung infection. Anat Rec (Hoboken) 293:968–981. https://doi.org/10.1002/ar.21094.
10. Marr HS, Edgell CJ. 2003. Testican-1 inhibits attachment of Neuro-2a cells. Matrix Biol 22:259–266. https://doi.org/10.1016/S0945-053X(03)00036-2.
11. Schnepp A, Komp Lindgren P, Hulsmann H, Kroger S, Paulsson M, Hartmann U. 2005. Mouse testican-2. Expression, glycosylation, and effects on neurite outgrowth. J Biol Chem 280:11274–11280. https://doi.org/10.1074/jbc.M414276200.
12. Yamamoto A, Uchiyama K, Nara T, Nishimura N, Hayasaka M, Hanaoka K, Yamamoto T. 2014. Structural abnormalities of corpus callosum and cortical axonal tracts accompanied by decreased anxiety-like behavior and lowered sociability in Spock3-mutant mice. Dev Neurosci 36:381–395. https://doi.org/10.1159/000363101.
13. Nakada M, Miyamori H, Yamashita J, Sato H. 2003. Testican 2 abrogates inhibition of membrane-type matrix metalloproteinases by other testican family proteins. Cancer Res 63:3364–3369.
14. Lewerenz M, Mogensen KE, Uze G. 1998. Shared receptor components but distinct complexes for alpha and beta interferons. J Mol Biol 282:585–599. https://doi.org/10.1006/jmbi.1998.2026.
15. Cutrone EC, Langer JA. 1997. Contributions of cloned type I interferon receptor subunits to differential ligand binding. FEBS Lett 404:197–202. https://doi.org/10.1016/s0014-5793(97)00129-4.
16. Moraga I, Harari D, Schreiber G, Uze G, Pellegrini S. 2009. Receptor density is key to the alpha2/beta interferon differential activities. Mol Cell Biol 29:4778–4787. https://doi.org/10.1128/MCB.01808-08.
17. Wang T, Liu X, Tian Q, Liang T, Chang P. 2018. Reduced SPOCK1 expression inhibits non-small cell lung cancer cell proliferation and migration through Wnt/beta-catenin signaling. Eur Rev Med Pharmacol Sci 22:637–644. https://doi.org/10.26355/eurrev_201802_14288.
18. Miao L, Wang Y, Xia H, Yao C, Cai H, Song Y. 2013. SPOCK1 is a novel transforming growth factor-beta target gene that regulates lung cancer cell epithelial-mesenchymal transition. Biochem Biophys Res Commun 440:792–797. https://doi.org/10.1016/j.bbrc.2013.10.024.
19. Hawkins F, Kramer P, Jacob A, Driver I, Thomas DC, McCauley KB, Skvir N, Crane AM, Kurmann AA, Hollenberg AN, Nguyen S, Wong BG, Khalil AS, Huang SX, Guttentag S, Rock JR, Shannon JM, Davis BR, Kotton DN. 2017. Prospective isolation of NKX2-1-expressing human lung progenitors derived from pluripotent stem cells. J Clin Invest 127:2277–2294. https://doi.org/10.1172/JCI89950.
20. Meh P, Pavsic M, Turk V, Baici A, Lenarcic B. 2005. Dual concentration-dependent activity of thyroglobulin type-1 domain of testican: specific inhibitor and substrate of cathepsin L. Biol Chem 386:75–83. https://doi.org/10.1515/BC.2005.010.
21. Xu X, Greenland JR, Gotts JE, Matthay MA, Caughey GH. 2016. Cathepsin L helps to defend mice from infection with influenza A. PLoS One 11:e0164501. https://doi.org/10.1371/journal.pone.0164501.
22. Coleman MD, Ha SD, Haeryfar SMM, Barr SD, Kim SO. 2018. Cathepsin B plays a key role in optimal production of the influenza A virus. J Virol Antivir Res 2018:1–20. https://doi.org/10.4172/2324-8955.1000178.
23. McCormick C, Duncan G, Goutsos KT, Tufaro F. 2000. The putative tumor suppressors EXT1 and EXT2 form a stable complex that accumulates in the Golgi apparatus and catalyzes the synthesis of heparan sulfate. Proc Natl Acad Sci U S A 97:668–673. https://doi.org/10.1073/pnas.97.2.668.
24. Senay C, Lind T, Muguruma K, Tone Y, Kitagawa H, Sugahara K, Lidholt K, Lindahl U, Kusche-Gullberg M. 2000. The EXT1/EXT2 tumor suppressors: catalytic activities and role in heparan sulfate biosynthesis. EMBO Rep 1:282–286. https://doi.org/10.1093/embo-reports/kvd045.
25. Busse M, Feta A, Presto J, Wilen M, Gronning M, Kjellen L, Kusche-Gullberg M. 2007. Contribution of EXT1, EXT2, and EXTL3 to heparan sulfate chain elongation. J Biol Chem 282:32802–32810. https://doi.org/10.1074/jbc.M703560200.
26. Aquino RS, Park PW. 2016. Glycosaminoglycans and infection. Front Biosci (Landmark Ed) 21:1260–1277.
27. Iozzo RV, Schaefer L. 2015. Proteoglycan form and function: a comprehensive nomenclature of proteoglycans. Matrix Biol 42:11–55. https://doi.org/10.1016/j.matbio.2015.02.003.
28. Zen K, Liu DQ, Li LM, Chen CX, Guo YL, Ha B, Chen X, Zhang CY, Liu Y. 2009. The heparan sulfate proteoglycan form of epithelial CD44v3 serves as a CD11b/CD18 counter-receptor during polymorphonuclear leukocyte transepithelial migration. J Biol Chem 284:3768–3776. https://doi.org/10.1074/jbc.M807805200.
29. WuDunn D, Spear PG. 1989. Initial interaction of herpes simplex virus with cells is binding to heparan sulfate. J Virol 63:52–58.
30. Brauer R, Ge L, Schlesinger SY, Birkland TP, Huang Y, Parimon T, Lee V, McKinney BL, McGuire JK, Parks WC, Chen P. 2016. Syndecan-1 attenuates lung injury during influenza infection by potentiating c-Met signaling to suppress epithelial apoptosis. Am J Respir Crit Care Med 194:333–344. https://doi.org/10.1164/rccm.201509-1878OC.
31. Bose S, Banerjee AK. 2002. Role of heparan sulfate in human parainfluenza virus type 3 infection. Virology 298:73–83. https://doi.org/10.1006/viro.2002.1484.
32. Dittmann M, Hoffmann HH, Scull MA, Gilmore RH, Bell KL, Ciancanelli M, Wilson SJ, Crotta S, Yu Y, Flatley B, Xiao JW, Casanova JL, Wack A, Bieniasz PD, Rice CM. 2015. A serpin shapes the extracellular environment to prevent influenza A virus maturation. Cell 160:631–643. https://doi.org/10.1016/j.cell.2015.01.040.
33. Ye L, Zhao B, Yuan K, Chu Y, Li C, Zhao C, Lian QQ, Ge RS. 2012. Gene expression profiling in fetal rat lung during gestational perfluorooctane sulfonate exposure. Toxicol Lett 209:270–276. https://doi.org/10.1016/j.toxlet.2011.12.013.
34. Morales Johansson H, Newman DR, Sannes PL. 2014. Whole-genome analysis of temporal gene expression during early transdifferentiation of human lung alveolar epithelial type 2 cells in vitro. PLoS One 9:e93413. https://doi.org/10.1371/journal.pone.0093413.
35. Nugent KM, Shanley JD. 1984. Verapamil inhibits influenza A virus replication. Arch Virol 81:163–170. https://doi.org/10.1007/BF01309305.
36. Fujioka Y, Tsuda M, Nanbo A, Hattori T, Sasaki J, Sasaki T, Miyazaki T, Ohba Y. 2013. A Ca(2+)-dependent signalling circuit regulates influenza A virus internalization and infection. Nat Commun 4:2763. https://doi.org/10.1038/ncomms3763.
37. Vannahme C, Schubel S, Herud M, Gosling S, Hulsmann H, Paulsson M, Hartmann U, Maurer P. 1999. Molecular cloning of testican-2: defining a novel calcium-binding proteoglycan family expressed in brain. J Neurochem 73:12–20. https://doi.org/10.1046/j.1471-4159.1999.0730012.x.
38. Turan K, Mibayashi M, Sugiyama K, Saito S, Numajiri A, Nagata K. 2004. Nuclear MxA proteins form a complex with influenza virus NP and inhibit the transcription of the engineered influenza virus genome. Nucleic Acids Res 32:643–652. https://doi.org/10.1093/nar/gkh192.
39. Zimmermann P, Manz B, Haller O, Schwemmle M, Kochs G. 2011. The viral nucleoprotein determines Mx sensitivity of influenza A viruses. J Virol 85:8133–8140. https://doi.org/10.1128/JVI.00712-11.
40. Goodman AG, Smith JA, Balachandran S, Perwitasari O, Proll SC, Thomas MJ, Korth MJ, Barber GN, Schiff LA, Katze MG. 2007. The cellular protein P58IPK regulates influenza virus mRNA translation and replication through a PKR-mediated mechanism. J Virol 81:2221–2230. https://doi.org/10.1128/JVI.02151-06.
41. Li Y, Banerjee S, Wang Y, Goldstein SA, Dong B, Gaughan C, Silverman RH, Weiss SR. 2016. Activation of RNase L is dependent on OAS3 expression during infection with diverse human viruses. Proc Natl Acad Sci U S A 113:2241–2246. https://doi.org/10.1073/pnas.1519657113.
42. Brass AL, Huang IC, Benita Y, John SP, Krishnan MN, Feeley EM, Ryan BJ, Weyer JL, van der Weyden L, Fikrig E, Adams DJ, Xavier RJ, Farzan M, Elledge SJ. 2009. The IFITM proteins mediate cellular resistance to influenza A H1N1 virus, West Nile virus, and dengue virus. Cell 139:1243–1254. https://doi.org/10.1016/j.cell.2009.12.017.
43. Diamond MS, Farzan M. 2013. The broad-spectrum antiviral functions of IFIT and IFITM proteins. Nat Rev Immunol 13:46–57. https://doi.org/10.1038/nri3344.